OncoTargets and Therapy

Dovepress
open access to scientific and medical research

Open Access Full Text Article

ORIGINAL RESEARCH

RETRACTED ARTICLE: MLPH Accelerates the Epithelial–Mesenchymal Transition in Prostate Cancer

This article was published in the following Dove Press journal:
OncoTargets and Therapy

Tianbiao Zhang*
Yangyang Sun*
Tao Zheng
Rui Wang
Donghui Jia
Weixing Zhang

Department of Urology, The First Affiliated Hospital of Zhengzhou University, Zhengzhou 450052, People's Republic of China

*These authors contributed equally to this work

Introduction: Prostate cancer (PC) is the second greatest cause of cancer deaths globally. PC presents a poor prognosis once it metastasizes. There is considerable proof of vital epithelial–mesenchymal transition (EMT) functionality in PC metastasis. Previous studies revealed that melanophilin (MLPH) is associated with PC; however, its role in PC remains poorly understood.

Methods: Bioinformatics analyses were performed. The cellular responses to MLPH knockdown were examined in HCC cell lines via wound healing assay, migration and invasion assay, Western blotting.

Results: Analysis of the PRCA GeneV2 database revealed that high MLPH expression might indicate poor overall survival. MLPH knockdown reduced PC cell migration, proliferation, and invasion. MLPH downregulation in vivo resulted in a lower growth rate and fewer metastatic nodules in lung tissues. Furthermore, MLPH knockdown recovered downregulated expression of the mesenchymal marker N-cadherin and the epithelial marker E-cadherin following a decrease in β-catenin.

Conclusion: These results indicate that progression of PC is stimulated via MLPH-dependent initiation of the EMT.

Keywords: MLPH, epithelial-to-mesenchymal transition, prostate cancer, β-catenin

Introduction

Prostate cancer (PC) ranks as the second most prevalent tumor in men, and in some regions ranks first,[1] with sources predicting 358,989 deaths and 1,276,106 new cases in 2018.[2] Metastasized tumors result in dramatically reduced survival rates.[3] This has necessitated a better understanding of the mechanisms of PC development and progression.

The epithelial–mesenchymal transition (EMT) initiates and significantly regulates progression and metastasis of PC.[4] An intricate procedure, the EMT triggers alterations in epithelial cell plasticity via transient de-differentiation into a mesenchymal phenotype.[5] The EMT is one of the primary means of cancer cell metastasis. A previous study revealed that a melanophilin (MLPH) variant was associated with PC.[6] Mancuso et al also reported that MLPH was associated with PC risk.[7] Bu et al revealed a higher level of MLPH in prostate tissue.[8] Conducive microenvironments for the progression and metastasis of PC are orchestrated via β-catenin signaling.[9] Therefore, we hypothesized that MLPH is involved in the EMT due to the potential association of MLPH with PC progression. This study aimed to investigate the role of MLPH in PC, as it remains particularly ambiguous.

Correspondence: Weixing Zhang
Department of Urology, The First Affiliated Hospital of Zhengzhou University, Zhengzhou 450052, People's Republic of China
Email caolingdudu@126.com

submit your manuscript | www.dovepress.com
DovePress
http://doi.org/10.2147/OTT.S225023

Materials and Methods

Bioinformatics Analysis

The PROGgeneV2 Pan Cancer Prognostics Database (http://genomics.jefferson.edu/proggene/) was used to analyze the role of MLPH in PC.[10]

Cell Culture

The PC cell lines PC3 and LNCaP were purchased from the American Type Culture Collection (Manassas, VA, USA). These cells were cultured in RPMI-1640 medium (Sigma-Aldrich, Shanghai, China) with the addition of 10% fetal bovine serum (FBS; Invitrogen Gibco, New Zealand).

Colony Formation Assay

The colony formation assay was performed as described previously.[11] Briefly, stably infected cells were cultured in a 6-well plate at 500 cells/well. Cells were cultured for 2 weeks. Next, cells were fixed for 30 min with 10% formalin and stained with Giemsa for 3 min. The number of colonies with > 50 cells was recorded.

Quantitative Real-Time Reverse Transcription Polymerase Chain Reaction (RT-qPCR)

Total RNA was extracted using TRIzol reagent (Invitrogen). In accordance with the manufacturer's protocols, a reverse transcription system kit was used to synthesize the cDNA (Toyobo, Osaka, Japan). RT-qPCR was carried out using an ABI PRISM 7100 sequence detection system (Applied Biosystems, Foster City, CA, USA). GAPDH was applied as an internal control with the following primers: (forward) 5′-GGAGCGAGATCCCTCCAAAAT-3′ and (reverse) 5′-GGCTGTTGTCATACTTCTCATGG-3′. The primer sequences for MLPH were as follows: (forward) 5′-AAGCCCGCTTCAAGAGGTTC-3′ and (reverse) 5′-TGGTCGCTGTCTCCACTTCT-3′.

Western Blot (WB) Analysis

We extracted total protein using a radioimmunoprecipitation buffer kit (Sigma-Aldrich) and determined the protein concentration using a BCA protein assay kit (Beyotime, Shanghai, China). The proteins were separated by 8–12% sodium dodecyl sulfate polyacrylamide gel electrophoresis and transferred to a polyvinylidene fluoride membrane. Next, the membranes were blocked in 10% defatted milk for 2–3 h and incubated for at least 12 h at 4°C with GAPDH (1:1000; No. 5174, Cell Signaling Technology, Shanghai, China), MLPH (1:500; No. 10338-1-AP, Proteintech, Wuhan, China), N-cadherin (1:1000; No. ab76057, Abcam), total β-catenin (1:1000; No. 848, Cell Signaling Technology), E-cadherin (1:1000; No. ab76319, Abcam), and activated β-catenin (1:1000; No. 19807, Cell Signaling Technology) antibodies. The secondary antibody horseradish peroxidase-conjugated IgG (1:8000, Proteintech) was then applied for 1 h at 37°C. GAPDH was used as the internal control for all WB assays. The internal control for nuclear protein was Histone H3. Bio-Rad Quantity One software (Bio-Rad, Hercules, CA, USA) was used to analyze protein expression.

Lentiviral Infection

The lentiviral short hairpin RNA (shRNA) for MLPH was obtained commercially (Table 1, SHCLNV-NM_024101, Sigma-Aldrich). The oligonucleotides were phosphorylated, annealed, and cloned into the pLKO.1 vector. Viral infection was carried out according to the manufacturer's instructions. First, the cells were cultured with polybrene (~ 4 μg/mL) and viral particles (1×10^8). The medium was changed after 24 h. After 48 h, infected cells were screened for 7 consecutive days using puromycin (~ 1 μg/mL) to obtain stable cell lines with downregulation of MLPH. The levels of MLPH were detected by RT-qPCR and WB assay. These cells were used in subsequent experiments.

Wound Healing Assay

The cells were cultured in a 6-well plate until 100% confluence. A wound was produced by drawing a straight line with a pipette tip (10 μL). Subsequently, the cells were cultured in RPMI-1640 medium without FBS. AZD5153 is a novel bromodomain-containing protein 4 inhibitor. Following previous studies,[12,13] 100 nM AZD5135 (Medkoo Bioscience, Beijing, China), an inhibitor of proliferation, was included as a control group. After 24 h, the width of cell migration was recorded.

Transwell Migration Assay

A total of 1×10^5 cells was seeded into the upper chamber of the transwell unit with 200 μL of medium. Medium supplemented with 1% FBS (~ 500 μL) was added into the lower chamber. The non-migrating cells were wiped with cotton swabs after 1 day, and the cells on the lower side of the membrane were fixed with 10% formalin. The migrated cells were stained with 0.1% crystal violet.

Transwell Invasion Assay

First, Matrigel (BD Biosciences, Shanghai, China) was added to the upper chamber. Then, approximately 3 × 10^5 cells were seeded on top of the Matrigel with 250 μL medium without FBS. The lower chamber was filled with 800 μL medium with 1% FBS acting as a chemotactic factor. After 1 day, the cells in the upper chamber were fixed with 10% formalin. Non-invasive cells were gently wiped from the top of the Matrigel. The fixed cells were stained with crystal violet and counted.

In vivo Study

All of the animal studies were approved by the Animal Care and Use Committee of the First Affiliated Hospital of Zhengzhou University and were performed following the National Institutes of Health Guide for the Care and Use of Laboratory Animals.[14]

For in vivo xenograft studies, 15 mice were randomized into three groups. Approximately 2.5 × 10^6 PC3 sh-nc, 2.5 × 10^6 PC3 sh1, or 2.5 × 10^6 PC3 sh2 cells suspended in 200 μL of phosphate-buffered saline (PBS) were injected subcutaneously into each mouse. Tumor sizes were observed and calculated using the formula (0.5236 × length × width × depth) as previously described[3].

For the in vivo pulmonary metastasis model, approximately 1.5 × 10^6 PC3 sh-nc, 1.5 × 10^6 PC3 sh1, 1.5 × 10^6 PC3 sh2 cells suspended in 150 μL of PBS were injected via the tail vein in nude mice (20 g). At 4 weeks after injection, the mice were sacrificed and their lungs were observed. The number of pulmonary metastases on the surface was counted.

Statistical Analysis

Statistical analyses were performed using SPSS 17.0. All experiments were carried out at least in triplicate. The data are expressed as the means ± standard deviations. We evaluated statistical significance by Student's *t*-test or one-way analysis of variance. *P*-values ≤ 0.05 were considered to indicate statistical significance.

Results

High MLPH Expression Indicates a Decreased Overall Survival Trend

As per the prognostic PROGgeneV2 database evaluation (Figure 1), there was no noteworthy variance in the

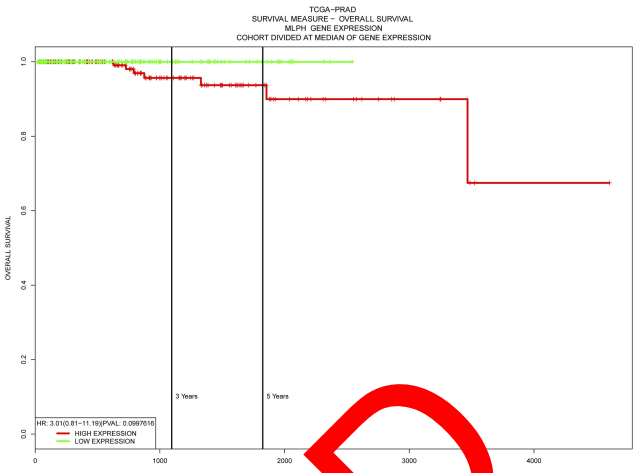

Figure 1 Analysis of the PROGgeneV2 prognostic database. Overall survival curves of patients with high and low melanophilin (MLPH) mRNA expression. Statistical analysis was performed using the log-rank test.

5-year survival rate between the low and high MLPH groups (low MLPH, n = 206; high MLPH, n = 207; hazard ratio, 3.01; 95% confidence interval (0.81–11.19); *P*-value = 0.09976). However, Figure 1 clearly shows a decreasing trend in overall survival in the high MLPH expression group.

Knockdown of MLPH Expression in PC3 and LNCaP Cells Using Lentiviral RNA Interference Vectors

Steady knockdown of MLPH expression in human PC cell lines (PC3 and LNCaP) using lentiviral RNA interference vectors that expressed shRNA (sh-MLPH) was used to examine the correlation between PC and MLPH. Protein and MLPH mRNA levels were assessed 5 days after lentiviral infection (Figure 2A and B), and a comparison with the control groups revealed that shRNA downregulated MLPH expression.

MLPH Knockdown Diminishes Proliferation, Migration, and Invasion of PC Cells

MLPH knockdown decreased cell proliferation at day 14 (Figure 3A), as assessed via the colony formation assay. Cell invasion and migration were also examined and were significantly reduced by MLPH knockdown; fewer cells were seen to migrate through the pores at 24 h, as shown in Figure 3B and C. Following a previous study,[12] an inhibitor of proliferation (AZD5135, 100 nM) was included as a control group.

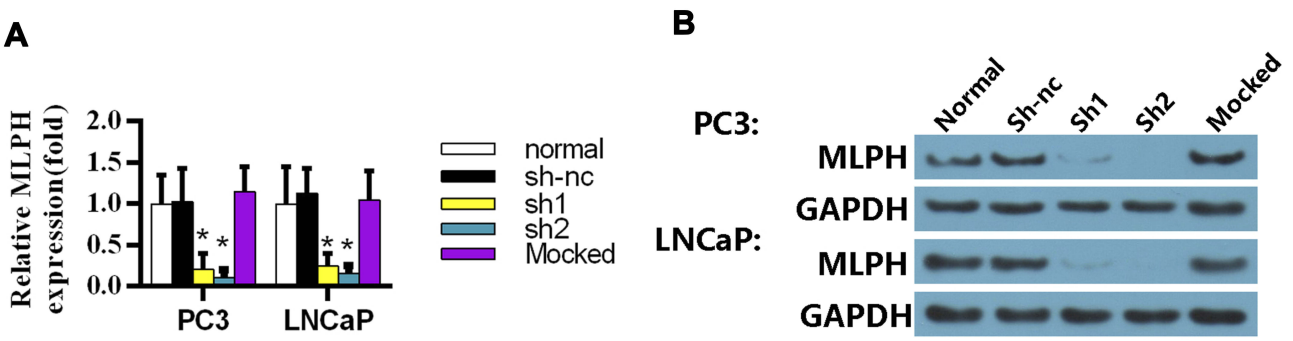

Figure 2 Establishment of MLPH-knockdown cells. (**A**) MLPH mRNA levels were analyzed via RT-qPCR. (**B**) Protein expression of MLPH was analyzed via Western blotting. Data are presented as means ± standard deviation. Each experiment was repeated at least five times with normal, negative control short hairpin RNA (sh-nc), short hairpin RNA1 (sh1), short hairpin RNA2 (sh2), and mock-treated (mocked) groups. *$P < 0.05$ compared to the sh-nc group.

A healing assay at 24 h revealed that the wound-closure ability of the PC cell lines was considerably diminished due to MLPH exhaustion (Figure 3D). MLPH knockdown significantly increased the migration of PC cells.

MLPH Knockdown Impairs Tumor Proliferation and Pulmonary Metastasis in vivo

In a tumor-transplant model, the effect of MLPH knockdown in PC was examined in vivo, and growth rates were reduced when MLPH levels were inhibited (Figure 4A and B). MLPH function in the metastasis of PC cells was also established in vivo via injection of MLPH into tail veins of nude mice. MLPH-knockdown hematoxylin and eosin (H&E)-stained pulmonary tissues exhibited fewer metastatic nodules in comparison to those in the sh-nc group (Figure 4C).

MLPH Knockdown Attenuates the EMT in PC Cell Lines

The EMT functions as a critical molecular marker when probing cancer behavior. Therefore, WB analyses of mesenchymal markers (N-cadherin and Vimentin) and epithelial (E-cadherin) markers revealed a sharp contrast, as MLPH knockdown downregulated N-cadherin and Vimentin and upregulated E-cadherin expression in PC cells (Figure 5). Moreover, both total and activated β-catenin were inhibited due to MLPH depletion (Figure 5).

Discussion

PC generally follows lung cancer as a leading cause of cancer deaths in males. In 2018, an estimated 1,276,106 PC patients were diagnosed, and 358,989 PC patients died.[2] Notably, if PC has metastasized, it cannot be cured.[1] With this in mind, definitive targets to improve PC prognosis and intervention efficacy are urgently needed.

MLPH is involved in the transport of melanosomes. Matesic et al observed upregulated MLPH levels in epithelial-enriched tissues, and MLPH mutations could trigger melanosome transport defects, as observed in Leaden mice.[3] Several studies have reported that MLPH expression is related to PC. Penney et al detected a significant association of PC risk variants with the expression of neighboring MLPH genes via the Affymetrix GeneChip,[6] and Nicholas et al established a correlation of MLPH with PC risk via a large-scale transcriptome-wide association study.[7] Moreover, based on the PROGgeneV2 prognostic database, we found that high MLPH expression is a predictor of poor overall survival. Thereafter, when investigating the role of MLPH in the progression and development of PC, we observed a decline in cell proliferation, migration, and invasion capability of PC cells when MLPH was downregulated. These results are similar to those of previous studies.[16,17]

Initially, the EMT occurs during early gastrulation and neural crest development.[18] The EMT causes epithelial cell alterations, so that they function similar to mesenchymal cells.[19] The EMT has been reported to play a critical role in metastasis.[20] The EMT entails tumor cells loosing surface contact and epithelial physiognomies during early metastasis phases, acquiring mesenchymal traits instead, which facilitates surrounding tissue invasion and metastasis.[21] During PC progression,

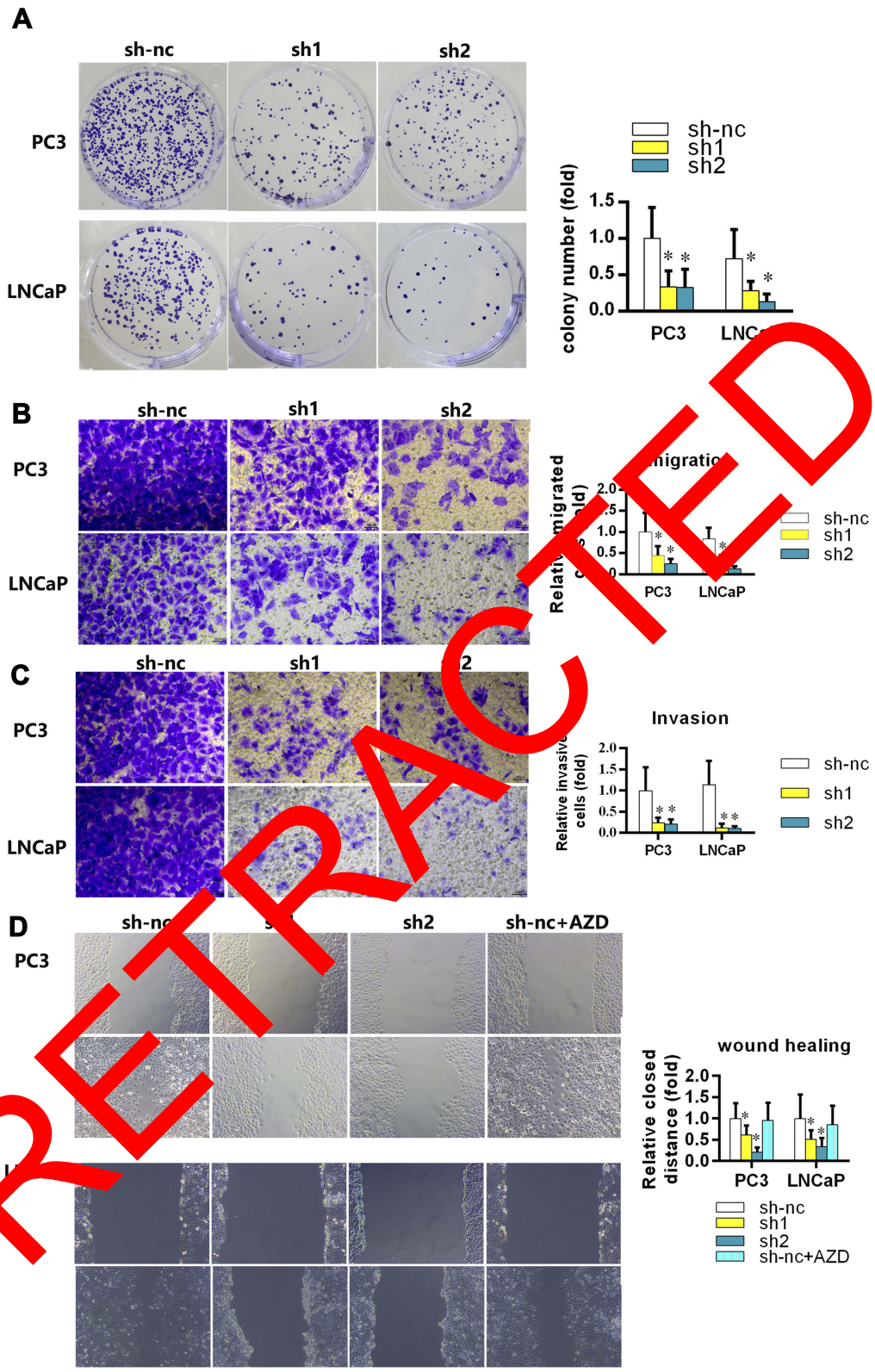

Figure 3 MLPH knockdown decreased proliferation, migration, and invasion of PC cell lines. (**A**) Effects of MLPH on cell proliferation were evaluated via colony formation assay at day 14 in PC3 and LNCaP cells. **P* < 0.05 compared to the sh-nc group. All data are expressed as means ± standard deviation. (**B**) Transwell migration assay was performed at 24 h to assess cell migration capabilities. The number of cells was counted, with six microscopic fields tallied per insert (magnification: 200×). **P* < 0.05 compared to the sh-nc group. All data are expressed as means ± standard deviation. (**C**) Transwell invasion assay was performed at 24 h to assess cell invasion capabilities. The number of cells was counted, with six microscopic fields per insert (magnification: 200×). **P* < 0.05 compared to the sh-nc group. All data are expressed as means ± standard deviation. (**D**) Wound healing assay was performed at 24 h to evaluate cell migration (magnification: 200×). Sh-nc+AZD: sh-nc group treated with AZD5135 (100 nM). The images are representative of five independent experiments. Relative widths of the wound gaps were measured using ImageJ software. All data are expressed as means ± standard deviation. **P* < 0.05 compared to the sh-nc group.

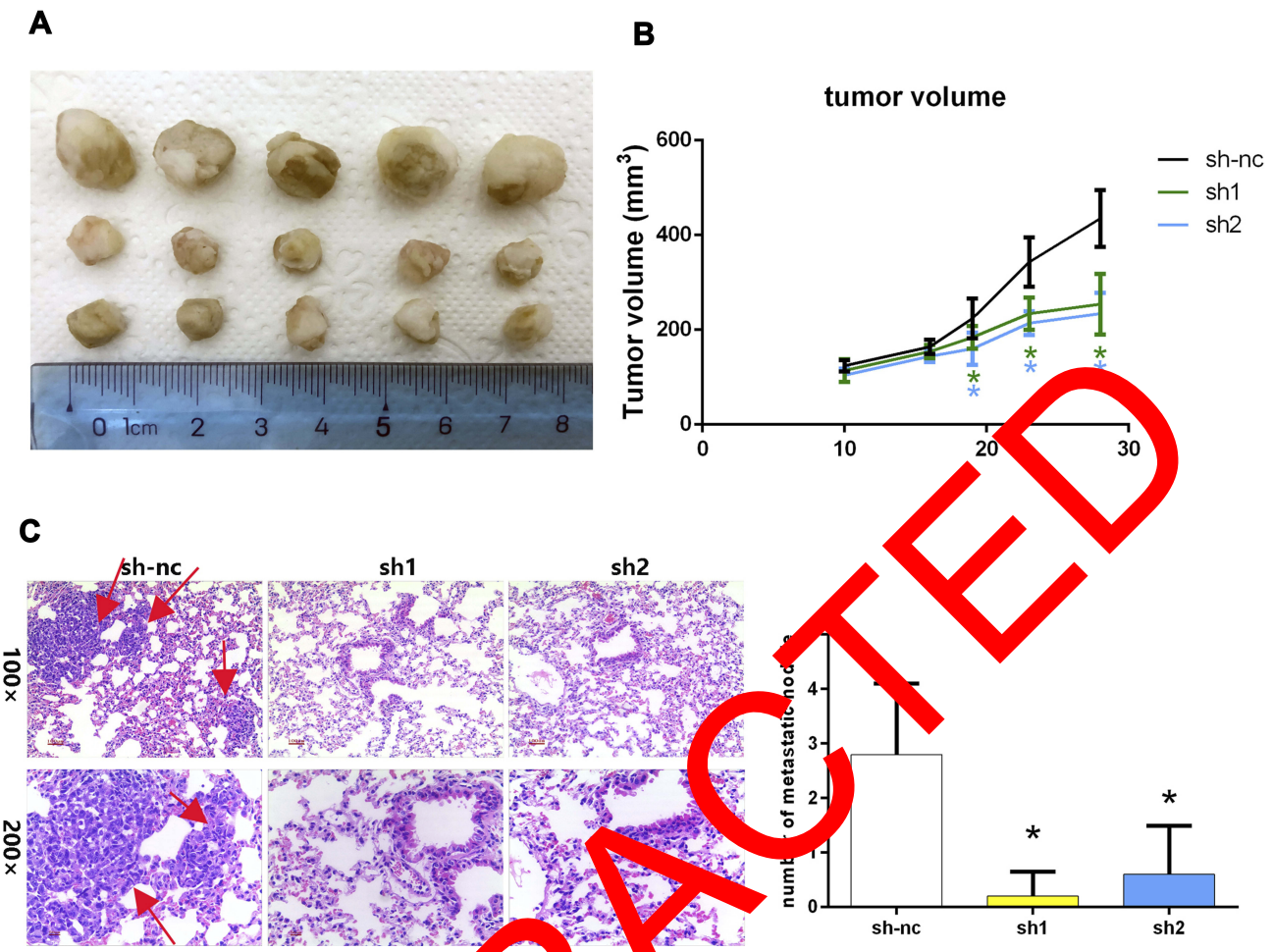

Figure 4 Depletion of MLPH decreased growth and lung metastasis in PC3 cells. (**A**) Gross photos of tumor tissues were obtained on day 28. (**B**) Tumor volume was gauged at days 10, 16, 19, 23, and 28. (**C**) Hematoxylin and eosin-stained lung sections were taken and the number of pulmonary metastatic nodules per lung tissue sample was calculated (n = 6). All data are expressed as mean ± standard deviation. *$P < 0.05$ compared to the sh-nc group; sh-nc, negative control short hairpin RNA; sh1, short hairpin RNA1; sh2, short hairpin RNA2.

epithelial cells undergo the EMT, characterized by morphological changes in their phenotype from cuboidal to spindle-shaped.[22] Epithelial cells predominantly express E-cadherin, whereas N-cadherin is a mesenchymal protein. Vimentin, a cytoskeleton protein, has been linked to initiation of the EMT. A previous study reported that a specific N-cadherin antibody could inhibit EMT progression while simultaneously reducing tumor growth invasion and migration in PC.[24] In this study, we observed increased E-cadherin and diminished N-cadherin and Vimentin expression as a result of MLPH depletion, thus implying the expression of MLPH in the EMT of PC cells.

PC cells hijack the EMT process to become invasive and migratory and acquire the ability to breakdown the basement membrane and metastasize. Wnt/β-catenin signaling, which has been implicated in control of the EMT, is correlated with the invasive and proliferative potencies of PC cells, as well as EMT traits.[25] Upregulation of β-catenin in PC cells antagonizes the EMT inhibition effect.[26] Liu et al reported that FOXO3 also suppresses the EMT via downregulation of β-catenin expression in PC cells.[9] Likewise, we observed decreased expression of total and activated β-catenin via silencing of MLPH. Thus, MLPH can upregulate the EMT induced by β-catenin activation in PC cells.

There are several limitations of this study. The in vitro outcomes must first be verified in both primary cells and PC cell lines. Second, stage-wise MLPH expression variations are yet to be established. Additional research is needed to establish the PC biomarker potential of MLPH expression.

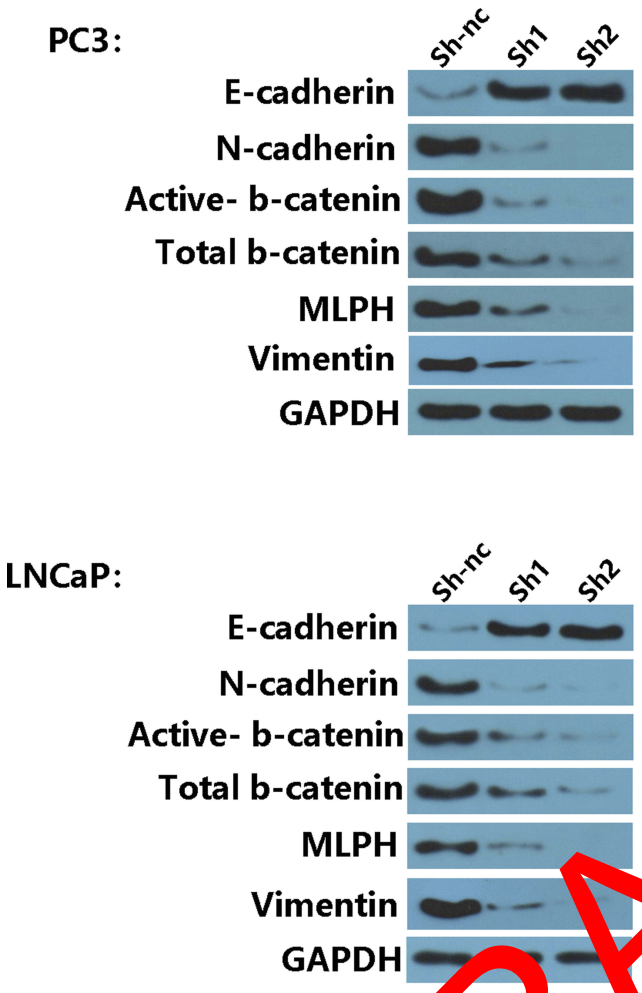

Figure 5 MLPH knockdown downregulated epithelial-to-mesenchymal transition (EMT) markers and β-catenin expression. (**A**) Images are representative of three independent experiments. Protein levels of E-cadherin, N-cadherin, Vimentin, MLPH, activated β-catenin, and total β-catenin were assessed via Western blotting. (**B**) Images are representative of three independent experiments.

Conclusions

The results of this study comprehensively specify inhibition of the EMT via MLPH knockdown in PC cells.

Abbreviations

PC, Prostate cancer; EMT, epithelial-to-mesenchymal transition; MLPH, Melanophilin; WB, Western blot; RT-qPCR, Real-time quantitative polymerase chain reaction; shRNA, short hairpin RNA.

Ethics Approval and Consent to Participate

The present study was approved by the Animal Care and Use Committee of The First Affiliated Hospital of Zhengzhou University.

Data Sharing Statement

The datasets used in this study are available from the corresponding author upon reasonable request.

Author Contributions

All authors contributed to data analysis, drafting and revising the article, gave final approval of the version to be published, and agree to be accountable for all aspects of the work.

Funding

This study was supported by the Henan Medical Scientific and Technological Project (172102310013, 201602006).

Disclosure

The authors declare that they have no competing interests.

References

1. Brody H. Prostate cancer. *Nature*. 2015;528:S117. doi:10.1038/528S117a
2. Bray F, Ferlay J, Soerjomataram I, Siegel RL, Torre LA, Jemal A. Global cancer statistics 2018: GLOBOCAN estimates of incidence and mortality worldwide for 36 cancers in 185 countries. *CA Cancer J Clin*. 2018;68:394–424. doi:10.3322/caac.21492
3. Eiberkorn U, Eder M, Kopka K, Babich JW, Eisenhut M. New strategies in prostate cancer: prostate-Specific Membrane Antigen (PSMA) ligands for diagnosis and therapy. *Clin Cancer Res*. 2016;22:9–15. doi:10.1158/1078-0432.CCR-15-0820
4. Chen WY, Tsai YC, Yeh HL, et al. Loss of SPDEF and gain of TGFBI activity after androgen deprivation therapy promote EMT and bone metastasis of prostate cancer. *Sci Signal*. 2017;10. doi:10.1126/scisignal.aam6826
5. Giannelli G, Koudelkova P, Dituri F, Mikulits W. Role of epithelial to mesenchymal transition in hepatocellular carcinoma. *J Hepatol*. 2016;65:798–808. doi:10.1016/j.jhep.2016.05.007
6. Penney KL, Sinnott JA, Tyekucheva S, et al. Association of prostate cancer risk variants with gene expression in normal and tumor tissue. *Cancer Epidemiol Biomarkers Prev*. 2015;24:255–260. doi:10.1158/1055-9965.EPI-14-0694-T
7. Mancuso N, Gayther S, Gusev A, et al. Large-scale transcriptome-wide association study identifies new prostate cancer risk regions. *Nat Commun*. 2018;9:4079. doi:10.1038/s41467-018-06302-1
8. Bu H, Narisu N, Schlick B, et al. Putative prostate cancer risk SNP in an androgen receptor-binding site of the melanophilin gene illustrates enrichment of risk SNPs in androgen receptor target sites. *Hum Mutat*. 2016;37:52–64. doi:10.1002/humu.22909
9. Liu H, Yin J, Wang H, et al. FOXO3a modulates WNT/β-catenin signaling and suppresses epithelial-to-mesenchymal transition in prostate cancer cells. *Cell Signal*. 2015;27:510–518. doi:10.1016/j.cellsig.2015.01.001
10. Goswami CP, Nakshatri H. PROGgeneV2: enhancements on the existing database. *BMC Cancer*. 2014;14:970. doi:10.1186/1471-2407-14-970
11. Liang X, Liu T, Zhang W, Zhang K, Guo S, Liang J. Lentivirus-mediated knockdown of M-phase phosphoprotein 8 inhibits proliferation of colon cancer cells. *Biotechnol Appl Biochem*. 2017;64:911–917. doi:10.1002/bab.1504

12. Shen G, Chen J, Zhou Y, et al. AZD5153 inhibits prostate cancer cell growth in vitro and in vivo. *Cell Physiol Biochem*. 2018;50:798–809. doi:10.1159/000494244
13. Huang X, Zhu D, Lou Y. A novel anticancer agent, icaritin, induced cell growth inhibition, G1 arrest and mitochondrial transmembrane potential drop in human prostate carcinoma PC-3 cells. *Eur J Pharmacol*. 2007;564:26–36. doi:10.1016/j.ejphar.2007.02.039
14. Workman P, Aboagye EO, Balkwill F, et al. Guidelines for the welfare and use of animals in cancer research. *Br J Cancer*. 2010;102:1555–1577. doi:10.1038/sj.bjc.6605642
15. Matesic LE, Yip R, Reuss AE, et al. Mutations in Mlph, encoding a member of the Rab effector family, cause the melanosome transport defects observed in leaden mice. *Proc Natl Acad Sci U S A*. 2001;98:10238–10243. doi:10.1073/pnas.181336698
16. Sha J, Han Q, Chi C, et al. PRKAR2B promotes prostate cancer metastasis by activating Wnt/beta-catenin and inducing epithelial-mesenchymal transition. *J Cell Biochem*. 2018;119:7319–7327. doi:10.1002/jcb.27030
17. Dual effects of constitutively active androgen receptor and fulllength androgen receptor for N-cadherin regulation in prostatecancer. *Oncotarget*. 2017;8, 42:72008–72020. doi:10.18632/oncotarget.18270
18. Yang J, Weinberg RA. Epithelial-mesenchymal transition: at the crossroads of development and tumor metastasis. *Dev Cell*. 2008;14:818–829. doi:10.1016/j.devcel.2008.05.009
19. Zhang Q, Liu S, Parajuli KR, et al. Interleukin-17 promotes prostate cancer via MMP7-induced epithelial-to-mesenchymal transition. *Oncogene*. 2017;36:687–699. doi:10.1038/onc.2016.240
20. Thiery JP, Lim CT. Tumor dissemination: an EMT affair. *Cancer Cell*. 2013;23:272–273. doi:10.1016/j.ccr.2013.03.004
21. Sjoberg E, Meyrath M, Milde L, et al. A novel ACKR2-dependent role of fibroblast-derived CXCL14 in epithelial-to-mesenchymal transition and metastasis of breast cancer. *Clin Cancer Res*. 2019;25:3702–3717. doi:10.1158/1078-0432.CCR-18-1294
22. Odero-Marah V, Hawsawi O, Henderson V, Sweeney J. Epithelial-Mesenchymal Transition (EMT) and prostate cancer. *Adv Exp Med Biol*. 2018;1095:101–110. doi:10.1007/978-3-319-95693-0_6
23. Di Donato M, Cernera G, Migliaccio A, Castoria G. Nerve growth factor induces proliferation and aggressiveness in prostate cancer cells. *Cancers (Basel)*. 2019;11. doi:10.3390/cancers11060784
24. Li P, Yang R, Gao WQ. Contributions of epithelial-mesenchymal transition and cancer stem cells to the development of castration resistance of prostate cancer. *Mol Cancer*. 2014;13:55. doi:10.1186/1476-4598-13-55
25. Jiang YG, Luo Y, He DL, et al. Role of Wnt/beta-catenin signaling pathway in epithelial-mesenchymal transition of human prostate cancer induced by hypoxia-inducible factor-1alpha. *Int J Urol*. 2007;14:1034–1039. doi:10.1111/j.1442-2042.2007.01866.x
26. Chen L, Mai W, Chen M, et al. Arenobufagin inhibits prostate cancer epithelial-mesenchymal transition and metastasis by down-regulating beta-catenin. *Pharmacol Res*. 2017;125:130–142. doi:10.1016/j.phrs.2017.07.009